Physics Faculty Publications   Physics Department

9-3-2007

Gigahertz Optical Spin Transceiver

Patrick Irvin

Petru S. Fodor
Cleveland State University, p.fodor@csuohio.edu

Jeremy Levy

Original Citation
Irvin, Patrick, Petru S. Fodor, and Jeremy Levy. "Gigahertz Optical Spin Transceiver." *Optics Express* 15 (2007): 11756-11762.

Gigahertz optical spin transceiver

Patrick Irvin[1]*, Petru S. Fodor[2], and Jeremy Levy[1]

[1]*Department of Physics and Astronomy, University of Pittsburgh, Pittsburgh, PA 15260*
[2]*Department of Physics, Cleveland State University, Cleveland, OH 44115*
*prist2@pitt.edu

Abstract: We present a time-resolved optical technique to measure electron spin dynamics with GHz dynamical bandwidth, transform-limited spectral selectivity, and phase-sensitive (lock-in) detection. Use of a continuous-wave (CW) laser and fast optical bridge enables greatly improved signal-to-noise characteristics compared to traditional optical sampling (pump-probe) techniques. We demonstrate the technique with a measurement of GHz-spin precession in n-GaAs. This approach may be applicable to other physical systems where stroboscopic techniques cannot be used because of either noise or spectral limitations.

References and links

1. S. A. Wolf, D. D. Awschalom, R. A. Buhrman, J. M. Daughton, S. von Molnar, M. L. Roukes, A. Y. Chtchelkanova, and D. M. Treger, "Spintronics: A spin-based electronics vision for the future," Science **294**, 1488-1495 (2001).
2. S. A. Crooker and D. L. Smith, "Imaging spin flows in semiconductors subject to electric, magnetic, and strain fields," Phys. Rev. Lett. **94**, 236601-236604 (2005).
3. R. J. Epstein, D. T. Fuchs, W. V. Schoenfeld, P. M. Petroff, and D. D. Awschalom, "Hanle effect measurements of spin lifetimes in InAs self-assembled quantum dots," App. Phys. Lett. **78**, 733-735 (2001).
4. X. Lou, C. Adelmann, S. A. Crooker, E. S. Garlid, J. Zhang, K. S. M. Reddy, S. D. Flexner, C. J. Palmstrom, and P. A. Crowell, "Electrical detection of spin transport in lateral ferromagnet-semiconductor devices," Nat. Phys. **3**, 197-202 (2007).
5. M. Oestreich, M. Romer, R. J. Haug, and D. Hagele, "Spin Noise Spectroscopy in GaAs," Phys. Rev. Lett. **95**, 216603-216604 (2005).
6. J. M. Kikkawa and D. D. Awschalom, "Resonant Spin Amplification in n-Type GaAs," Phys. Rev. Lett. **80**, 4313-4316 (1998).
7. F. T. Charnock, R. Lopusnik, and T. J. Silva, "Pump--probe Faraday rotation magnetometer using two diode lasers," Rev. Sci. Instrum. **76**, 056105-056103 (2005).
8. D. Gammon, E. S. Snow, B. V. Shanabrook, D. S. Katzer, and D. Park, "Fine Structure Splitting in the Optical Spectra of Single GaAs Quantum Dots," Phys. Rev. Lett. **76**, 3005-3008 (1996).
9. D. Magde, E. Elson, and W. W. Webb, "Thermodynamic Fluctuations in a Reacting System-Measurement by Fluorescence Correlation Spectroscopy," Phys. Rev. Lett. **29**, 705-708 (1972).
10. R. J. Kneisler, F. E. Lytle, G. J. Fiechtner, Y. Jiang, G. B. King, and N. M. Laurendeau, "Asynchronous optical sampling: a new combustion diagnostic for potential use in turbulent, high-pressure flames," Opt. Lett. **14**, 260-262 (1989).
11. J. J. Baumberg, S. A. Crooker, D. D. Awschalom, N. Samarth, H. Luo, and J. K. Furdyna, "Ultrafast Faraday spectroscopy in magnetic semiconductor quantum structures," Phys. Rev. B **50**, 7689-7700 (1994).

1. Introduction

Electron spin in semiconductors [1] has been extensively measured using a variety of techniques including Kerr rotation (KR) [2], Hanle effect [3], electrical detection with ferromagnetic electrodes [4], and noise spectroscopy [5]. The spin dynamics in these systems have generally been studied using stroboscopic techniques which utilize the temporal properties of mode-locked [6] or pulsed diode lasers [7].

Ultrafast spectroscopy provides exceptional time resolution, but there are drawbacks to the stroboscopic pump-probe approach for some investigations. Ultrashort optical pulses are limited in their spectral resolution by the time-energy uncertainty relation ($\Delta E \cdot \Delta t \geq \hbar$). High

spectral resolution becomes particularly important if one is interested in probing the dynamics of a system with sharp optical transitions, such as semiconductor quantum dots or defect states, without influence or disturbance from nearby systems. For example, pulses from a Ti:Sapphire laser with 150 fs pulsewidth at $\lambda = 750$ nm will have a transform-limited spectral width of $\Delta E \sim 50$ meV; by contrast, the linewidth of a typical quantum dot is less than 40 μeV [8]. A second, less fundamental limitation relates to acquisition of dynamics over long time scales comparable to the repetition rate for the experiment. Mechanical delay lines become cumbersome for pump-probe delays >5 ns; acquisition speed is limited by the rate at which these delay lines can be scanned. Other optical techniques that infer dynamics from continuous wave optical sources, for example fluorescence correlation spectroscopy [9], lack phase information that may be critical for some investigations.

While many of these limitations can be remedied by suitable choice of lasers, e.g., pulsed laser diodes with narrower spectra [7] and asynchronous optical sampling to address limitations associated with mechanical delay lines [10], there is a more subtle effect that impacts the signal-to-noise ratio (SNR) in stroboscopic or sampling experiments. In a typical pump-probe experiment the dynamics are sampled only for a small fraction of the interval in which the dynamics takes place. This fraction, $\Delta t / T$, where Δt is the sampling time and T is the period of the pulsed laser system, undersamples both the signal and any intrinsic noise (other than shot noise). In order to achieve an optimal SNR, it is advantageous to sample (hence average) the intrinsic noise as much as possible.
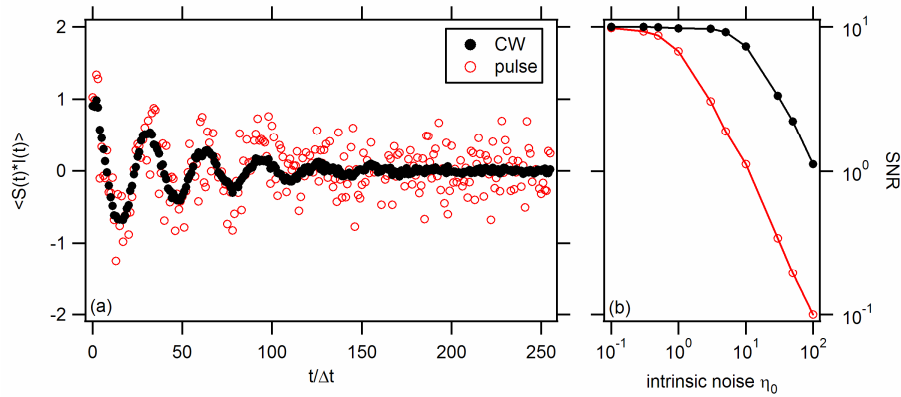

Fig. 1. Simulation of noise reduction when comparing a sampling technique (pulsed probe) with a continuous detection one (CW probe): (a) Averaged data for CW and stroboscopic acquisition. Here $S_0(t) = \exp(-T \cdot t) \cos(\omega \cdot t)$. The intrinsic noise is $\eta_0 = 0.3$ and the pulse width is $t_0 = 1$. (b) Comparison of SNR for CW and stroboscopic acquisition.

For purposes of illustration, one can assume that the signal of interest $S(t)$ is periodic with period T, and is sampled by an optical probe with intensity profile $I(t)$. One may consider two limiting cases where the optical profile is either constant ($I(t) = I_0$) or pulsed with a width t_0 ($I(t) = T / t_0 * I_0$, $0 < t < t_0$, and zero otherwise). Assuming that the intensity fluctuations in the optical signal are only limited by shot noise, one can model the physical system as $S(t) = S_0(t) + \eta(t)$, where $S_0(t)$ is a noise-free periodic function and $\eta(t)$ represents an intrinsic noise term (assumed here to be white: $\langle \eta(t) \cdot \eta(0) \rangle = \delta(t)$). The system is sampled by a shot-noise limited photon field $I(t)$, and the measured signal consists of averaging the product $S(t) * I(t)$ over many periods. Comparison of the two results [Fig. 1(a)] for the same number of measurement photons shows that continuous measurement

results in a maximum SNR improvement $\sim (T/\Delta t)^{1/2}$ over sampling methods, for the case where intrinsic noise dominates over shot noise [Fig. 1(b)].

Here we report on a realization of this approach to time-resolved optical detection based on the continuous detection method outlined above. Our approach utilizes a CW laser and high-bandwidth balanced photoreceiver to measure spin dynamics in semiconductors with superior noise characteristics compared to pump-probe (sampling) techniques. The functionality of this detection scheme is demonstrated by investigating spin dynamics in a well-studied sample, n-GaAs [6].
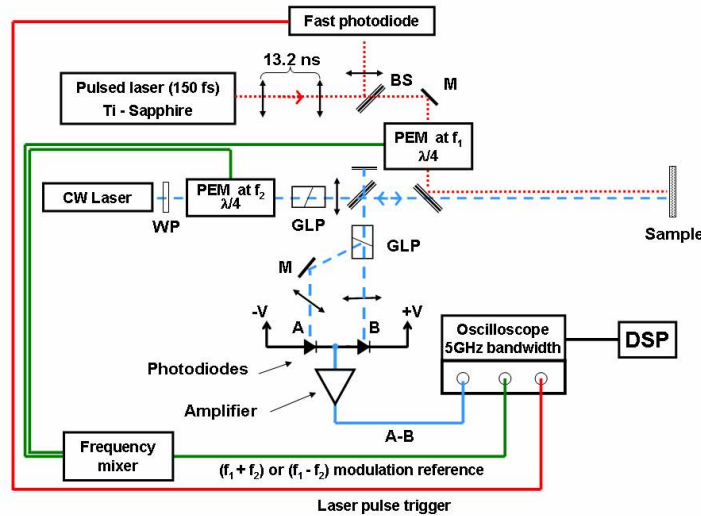

Fig. 2. (Color online) Schematic drawing of the experimental setup for the detection of electron spin coherence in semiconductors. (GLP) - Glan - Laser polarizer; (WP) – quarter wavelength plate; (PEM) – photoelastic modulators; (BS) – beamsplitters; (M) – mirrors; (DSP) - digital signal processor.

2. Principle of operation

2.1 Experimental set –up

In the investigation of spin dynamics in semiconductors, the Kerr effect provides direct information about the spin orientation. Upon reflection from a magnetic material, a linearly polarized laser will have its polarization direction rotated by an amount proportional to the magnetic moment along the propagation direction [11]. A diagram of our experiment is shown in Fig. 2. A pulsed laser is used to create a population of spin polarized electrons and a continuous-wave laser monitors the spin polarization by using the Kerr effect. In order to perform lock-in detection, the pump beam is modulated in helicity at frequency f_1 by a photoelastic modulator (*Hinds* PEM-90) to alternately create majority spin up and spin down electrons. The probe beam is intensity modulated with a PEM at frequency f_2. By tuning the probe wavelength one can measure the wavelength dependence of the Kerr signal. Additionally, this detection scheme also allows one to perform electro-optic measurements with comparable bandwidths.

A fast detector converts the polarization into an electrical signal that is then sent to a real-time, digitizing oscilloscope (*LeCroy* Wavemaster 8500A-VL) with 20 GS/s sampling rate. Oscilloscope acquisition is initiated by a pair of triggers: after first detecting a rising edge of the optical modulation ($f_r = f_r(f_1, f_2)$) the oscilloscope then triggers on the first detected

laser pulse. After being triggered, the oscilloscope simultaneously acquires two waveforms until the fast memory (32 MB) is filled, corresponding to 1.6 ms of continuous data. One waveform corresponds to the signal from the fast detector, while the other channel acquires a waveform representing the pump laser. This second waveform is necessary to determine the time of the pump events because the pump laser is not phase-locked to the sampling clock of the oscilloscope, as discussed in Section 2.2.

2.2 Digital signal processing

The 32 MB waveforms acquired by the detection electronics are transferred over gigabit Ethernet to a single processor Pentium PC (2.4 GHz clock speed, 2 GB memory), which performs the digital signal processing while the oscilloscope acquires the next dataset. The main steps of the digital processing algorithm implemented are: demodulation, time slicing, and averaging of the data.
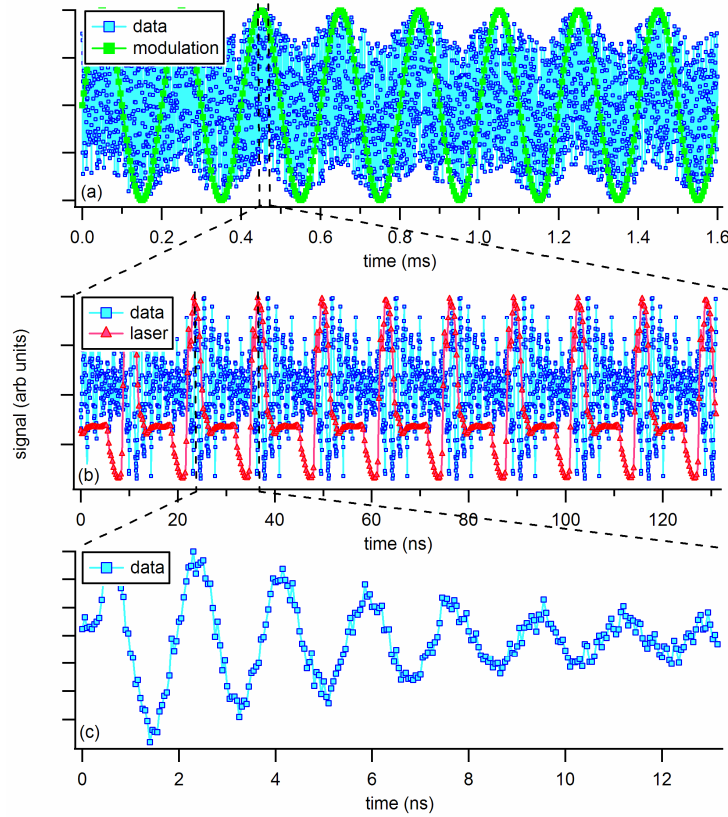

Fig. 3. (Color online) Data processing steps: (a) the acquired data is demodulated at the reference frequency f_r; (b) the independently acquired laser pulses are used as a reference for slicing the data waveform into segments equal with the excitation laser period; and (c) the resulting time-resolved Kerr rotation after processing 1.6 ms of acquired data.

As mentioned above, the pump and probe laser beams are modulated in polarization and intensity, respectively, allowing the implementation of a phase sensitive lock-in detection scheme by applying a Fourier decomposition method to the acquired time-dependent digital signal of $N = 32\,\mathrm{M}$ samples. For the frequency of interest, f_r, one can define a basis of square-integrable functions: $\tilde{X}_0(t) \equiv 1/\sqrt{2}$, $\tilde{X}_i(t) \equiv \cos(2\pi i f_r t)$, $i = 1,2,...$ and $\tilde{Y}_j(t) \equiv \sin(2\pi i f_r t)$,

$j = 1, 2, \ldots$, with the property that $\langle \tilde{X}_i | \tilde{Y}_j \rangle = 0$ and $\langle \tilde{X}_i | \tilde{X}_j \rangle = \langle \tilde{Y}_i | \tilde{Y}_j \rangle = \delta_{ij}$, where δ_{ij} is the Kronecker delta function. The Fourier decomposition of the signal then becomes

$$\tilde{S}(t) = \sum_{i=0}^{n} a_i \tilde{X}_i(t) + \sum_{i=0}^{n} b_j \tilde{Y}_j(t), \quad \text{where} \quad a_i = \langle \tilde{S} | \tilde{X}_i \rangle, \quad b_j = \langle \tilde{S} | \tilde{Y}_j \rangle \quad \text{and the upper limit}$$

$n = t_{samp} / (2 \cdot f_r)$, with the sampling period $t_{samp} = (20\,\text{GHz})^{-1} = 50\,\text{ps}$. In the simple case this allows the in- and out-of-phase components of the Kerr rotation at the reference frequency f_r to be extracted. The phase is determined by an autophase sequence similar to a conventional lock-in amplifier when the data is processed off-line.

For a typical pump laser repetition rate of 80 MHz and a data acquisition time of 1.6 ms, the sample is excited 128,000 times. Consequently, the acquired waveform contains an equivalent number of snapshots of the spin dynamics, with each time interval being approximately $T_L \approx 13\,\text{ns}$ long and digitized in $n_L \approx 250$ samples. Using the independently acquired waveform of the laser pulses, the demodulated data can be partitioned into one-period segments, which are averaged together [Fig. 3(c)] to produce a final waveform with 250 samples. The demodulation, time slicing, and averaging are thus equivalent to n_L parallel lock-in amplifiers. Therefore the speed at which dynamic data can be acquired is proportionally increased compared with traditional scanning mechanical delay stage, pump–probe experiments.

3. Experimental results

We have implemented our detection scheme to characterize the electron spin dynamics in n-GaAs (10^{16} cm^{-3} Si doped) epilayers. The sample was placed in the Voigt geometry in a magneto-optical cryostat which allows magnetic fields to be applied parallel to the sample surface. The sample was held at 15 K for the duration of the experiment. The electron spin direction is initialized with circularly polarized laser pulses (150 fs pulsewidth) generated by a mode locked Ti:Sapphire laser (50 mW), tuned above the bandgap of GaAs (815 nm). A linearly polarized continuous wave Ti: Sapphire laser (20 mW) is tuned to 822 nm to be near the absorption edge of GaAs. (Although our probe beam has a higher power than is generally used, the peak power is approximately five orders of magnitude less than when using femtosecond pulses.) The probe beam monitors the component of the electron spin magnetization along the light propagation direction. The time-dependent Kerr signal is detected using a pair of fast balanced photodiodes (*New Focus* Si 650 MHz balanced receiver). Demodulation was performed at the sum frequency: $f_r = f_1 + f_2$.

In a transverse magnetic field, the initialized electron spin population precesses around the magnetic field direction at the Larmor frequency, which is proportional to the magnetic field B and the electronic g factor. The instantaneous component of the electron population perpendicular to the magnetic field can be described by:

$$S_z(t) = A \exp(-t/T_1^*)\cos(\omega_L t) \qquad (1)$$

where A is the transversal magnetization of the electron spins at $t = 0$, $\omega_L = g\mu_B B / \hbar$ is the Larmor frequency, and an exponential envelope for the oscillatory signal is introduced to account for decoherence of the spin system with the inhomogeneous transverse dephasing time T_2^* [6].

Figure 4(a) depicts the Kerr rotation data recorded for the n-GaAs epilayers as a function of time and magnetic field. The magnetic field is swept from –200 to +200 mT in steps of 1 mT and 16 ms of data is acquired at each field step. The experimental data is in good agreement with simulated data obtained using $g = -0.41$ and a transverse spin decoherence time of $T_2 = 100$ ns. The small offset from zero field arises from trapped flux in the

superconducting magnet. In GaAs, the spin decoherence time is particularly long compared with the laser repetition rate so we have used a modified version of Eq. (1) [6]:

$$S_z(t) = \sum_{n_{probe}} \exp\left(-\left[t + n_{pulse}T_L\right]/T_2\right)\cos\left(\omega_L t + n_{pulse}T_L\right) \qquad (2)$$

This equation accounts for the polarization of the electron spin remaining beyond the 13 ns period between consecutive laser pulses.
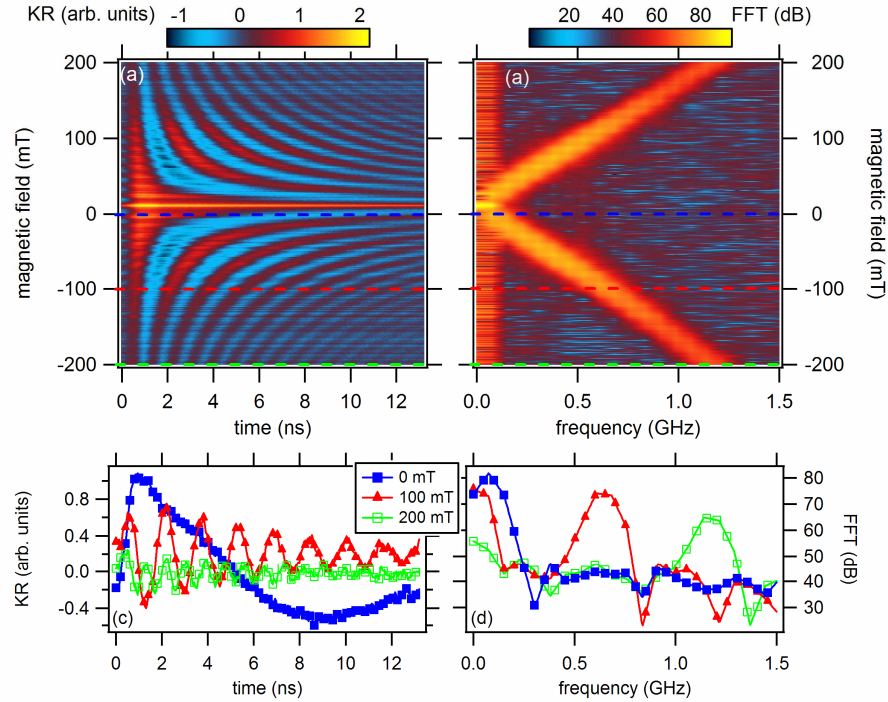

Fig. 4. (Color online) (a) Acquired Kerr rotation data for n-GaAs as a function of the delay time (horizontal axis) and external magnetic field (vertical axis); (b) Fast Fourier Transform (FFT) of the data giving the Larmor precession frequency as a function of the magnetic field; (c) Line cuts through the Kerr rotation plot at different magnetic fields (0, 100 and 200 mT); (d) Line cuts through the FFT data showing the resonant frequency for H = 0, 100 and 200 mT.

A consequence of this long decoherence time is the observation of resonant spin amplification at specific magnetic fields for which the Larmor precession frequency is commensurate with the laser repetition rate (Fig. 5) [6]. One of the experimental features not accounted for in the simulation is the higher intensity of the resonant spin amplification signal at $B = 0\,T$. However, in our simulation we have not considered the field dependence of the spin life time which for $n = 3 \times 10^{16}\,cm^{-3}$ doped GaAs decreases with increasing magnetic field [6].
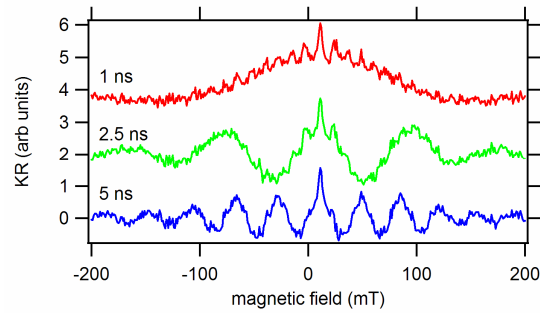
Fig. 5. (Color online) Kerr rotation as a function of magnetic field. Rapid oscillation visible at 1 ns is due to resonant spin amplification. Slow oscillations visible at 2.5 and 5 ns are due to changing precession frequency with field. Curves are offset for clarity.

The estimated speed of collecting and processing the information is similar to that of scanning mechanical delay pump-probe experiments. The major bottleneck in the presented implementation is the PCI architecture of the oscilloscope, in which the data stream requires a $T_r = 13\,\text{s}$ recovery time after each set of 1.6 ms segment of data is acquired by the fast memory in the oscilloscope. With the use of dedicated field programmable gate arrays (FPGA) for the DSP, the current architecture can be greatly improved by virtually eliminating the recovery time and increasing the efficiency by $T_r /(N \cdot T_{samp})$: a factor of 10^4 speedup for a given SNR.

4. Conclusion

In summary, we have presented a method for acquiring time-resolved optical signals using CW optical probes. Using this method, it is possible to work close to the time-energy uncertainty limit and obtain simultaneously high spectral selectivity and temporal resolution. This method is able to provide improved signal to noise characteristics compared to sampling techniques. With signal processing improvements, the method presented here may enable the real-time monitoring of electron spin dynamics in spectrally narrow systems, such as semiconductor quantum dots.

Acknowledgments